

Received September 12, 2019, accepted October 2, 2019, date of publication October 14, 2019, date of current version November 5, 2019.

Digital Object Identifier 10.1109/ACCESS.2019.2947196

# A Correction Model for the Continuous Deflection Measurement of Pavements Under Dynamic Loads

JIANGHAI LIAO<sup>1,2</sup>, HONG LIN<sup>3</sup>, QINGQUAN LI<sup>1,4</sup>, AND DEJIN ZHANG<sup>1,4</sup>

<sup>1</sup>Shenzhen Key Laboratory of Spatial Smart Sensing and Service, Shenzhen University, Shenzhen 518060, China

<sup>2</sup>School of Electronics and Information Engineering, Shenzhen University, Shenzhen 518060, China

<sup>3</sup>Wuhan Wuda Zoyon Science and Technology Co., Ltd., Wuhan 430223, China

<sup>4</sup>School of Architecture and Urban Planning, Shenzhen University, Shenzhen 518060, China

Corresponding author: Dejin Zhang (djzhang@whu.edu.cn)

This work was supported in part by the Nature Science Foundation of China under Grant 71961137003, and in part by the National Key Research and Development Programmes of China under Grant 2016YFB0502203.


**ABSTRACT** Pavement deflection is the primary indicator reflecting road-bearing capacity. The falling weight deflectometer (FWD) and the Benkelman beam deflectometer (BBD) are widely used in deflection measurement, and are suitable for measuring the elastic deflection of pavement under static loading or dynamic impact loading. In recent years, there has been an increasing interest in continuous dynamic deflectometers, especially velocity-based deflectometers. The velocity-based continuous dynamic deflectometers, such as the laser dynamic deflectometer (LDD), are used to solve the problems of traffic speed and non-destructive pavement deflection measurement. However, there can be many deviations caused by the varied environmental parameters in practical application. In this article, through the review of the mechanism of the Euler-Bernoulli beam upon an elastic foundation and the corresponding influencing factors, the internal and external factors causing dynamic deflection measurement deviation are analyzed and summarized. The influences of pavement temperature, vehicle speed, pavement condition, and other factors are summarized and discussed. On this basis, a model of environmental parameter correction for the continuous dynamic deflectometer is established using a regression analysis method. Numbers of experiments confirmed the reliability of the correction model under different measurement conditions. The correlation experiments between the LDD and different types of deflectometer confirmed the accuracy of the correction model under different measurement conditions. The results showed that the correction model for the continuous deflection measurement of pavements under dynamic loads has strong robustness in different environments and conditions.

**INDEX TERMS** Bearing capacity, non-destructive measurement, dynamic deflection, laser doppler, deflection correction.

## I. INTRODUCTION

Deflection is an important index reflecting the comprehensive bearing capacity of subgrade and pavement, which is influenced by the compacted material density [1] and material stiffness [2]. There are three typical methods of deflection measurement: (1) static load deflection measurement (e.g. the Benkelman beam deflectometer, BBD), which involves measuring the maximum deflection response of a pavement to static applied loads [3]; (2) dynamic impact deflection

measurement (e.g. the falling weight deflectometer, FWD), which involves measuring the maximum deflection response of a pavement to dynamic impact applied loads [4], [5]; and (3) continuous dynamic deflection measurement (e.g. the laser dynamic deflectometer, LDD), which involves measuring the maximum deflection response of a pavement under the continuous dynamic wheel load of vehicles [6]. Static load deflection measurement and dynamic impact deflection measurement are limited in practical application as they need sufficient response time for the deformation and recovery. As a result, these methods are low speed (1–5 km/h) and ineffective (10–50 m per sample point) [3]–[5]. Continuous dynamic

The associate editor coordinating the review of this manuscript and approving it for publication was Xiaokang Yin .

deflection measurement solves both problems and offers a much more reasonable process because it fits naturally to the way that pavement is actually used.

In recent years, there has been an increasing interest in continuous dynamic deflection measurement. Typical products are the rolling wheel deflectometer (RWD) [6], [7], the road deflection tester (RDT) [8], and the rolling dynamic deflectometer (RDD) [9], [10]. However, all these methods using force-displacement principle have been developed through laboratory experiments, and few have been applied in practical applications [11]–[13]. Greenwood Engineering of Denmark and ZOYON of China have developed methods based on the velocity-based measurement of pavement deformation and a theoretical model of the deflection value. They produce products such as the high-speed deflectograph (HSD), the traffic speed deflectometer (TSD), and the laser dynamic deflectometer (LDD), which have been successful in both theory and application [14]–[17]. However, a major problem with these deflectometers is the possible deviation of the external and internal environmental parameters of the dynamic deflection measurement. The result of the dynamic deflection value is influenced by the different correction coefficients for the dynamic load, vehicle speed, pavement roughness, pavement temperature, etc. To date, the existing research has mostly focused on qualitative research into these influencing factors, and there is a lack of theoretical models and data support.

The deflection caused by traffic load is not symmetric, as for stationary loads [15]–[17], and the deflection basin is expressed in the form of a curve that propagates in the driving direction. Following the theory of elastic wave propagation in solids, the dynamic deflection waves are related to the tendency of a material to maintain its shape and not deform whenever a force or stress is applied to it. Accordingly, dynamic deflection waves have additional influencing factors, such as the dynamic load, vehicle speed, pavement roughness, and pavement temperature. To date, most research has been focused on pavement temperature correction, where valuable research results have been obtained. The influence of pavement temperature on the measurement results is usually corrected by a temperature correction coefficient, in which the influencing factors of the different correction models are different [18]–[20]. The influencing factors include pavement temperature, asphalt layer thickness, modulus of resilience of the subgrade top surface, cracking state, type of subgrade material, and so on. The various models show the importance of temperature correction, and also reflect that it is difficult to obtain a unified model for temperature correction. Pavement roughness is another important factor, which is usually evaluated by the International Roughness Index (IRI). The Transport Research Laboratory (TRL) in the United Kingdom has reported that road roughness has a great influence on the TSD [21]. The existing deflection measurement products are mainly the FWD and the BBD, which differ from the continuous dynamic deflectometer. The measurement results have nothing to do with the measurement speed,

and the measurement load is relatively fixed. As a result, there has been little research on measurement speed and dynamic load correction. Previous research has evaluated the effect of vehicle speed on continuous dynamic deflection measurement based on the data of one subgrade pavement and two asphalt pavements [14], but further research is still needed.

This article presents an overview of the velocity-based continuous dynamic deflectometer. By using the deflection velocity of several sampling points, the deflection basin is inverted by linear regression and the initial deflection value is calculated. A calibration-based method is then used to achieve the calculation of the system parameters for the continuous dynamic deflectometer. Then, starting with the analysis of the mechanism of the LDD and the quantitative influencing factors, the potential main influencing factors are considered as the dynamic load, vehicle speed, pavement roughness, and pavement temperature.

Based on these findings, a recommended correction model for the environmental parameters of the continuous dynamic deflectometer is presented, the feasibility of which was confirmed by repeatability and correlation experiments. The results showed that the velocity-based method of the continuous dynamic deflectometer has strong robustness in different environments and conditions. As of March 2018, continuous dynamic deflectometers have completed 200,000 km of actual engineering measurement in China. The proposed correction method supports the continuous dynamic deflectometer at a normal traffic speed of 20–90 km/h, to meet the demands of network-level deflection measurement.

The rest of this paper is organized as follows. Section II reviews the related work. Section III describes the correction of the system parameters for the continuous dynamic deflectometer. Section IV presents the repeatability verification and correlation verification. Finally, Section V provides a summary of the work.

## II. RELATED WORK

The model of the Euler-Bernoulli beam on an elastic foundation is used to solve the problem of traffic speed and non-destructive pavement deflection measurement. By measuring the deflection velocity in predetermined positions of the deflection basin, the deflection value can be obtained.

### A. PRINCIPLE OF DYNAMIC DEFLECTION MEASUREMENT BASED ON DEFLECTION VELOCITY

The structural layers of an asphalt pavement (including the surface layer, base layer, and cushion layer) are simplified as an arbitrary (possibly infinite) long beam on an elastic foundation. The axle load is applied at the beam and creates a deflection basin. Figure 1a depicts how an ideal elastic material deforms, which is usually in proportion to the applied axle load and recovers when the load wheel is leaving. Figure 1b shows that the dynamic deflection wave is a mechanical

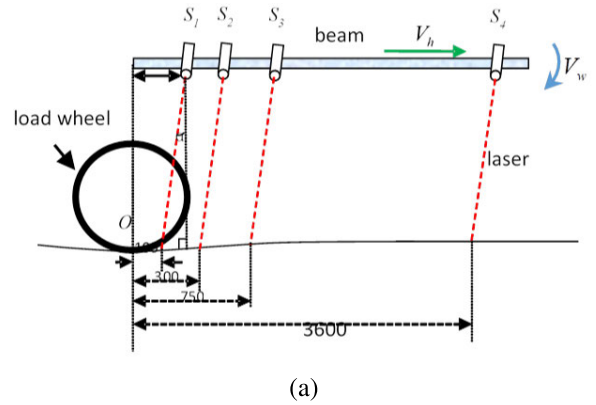
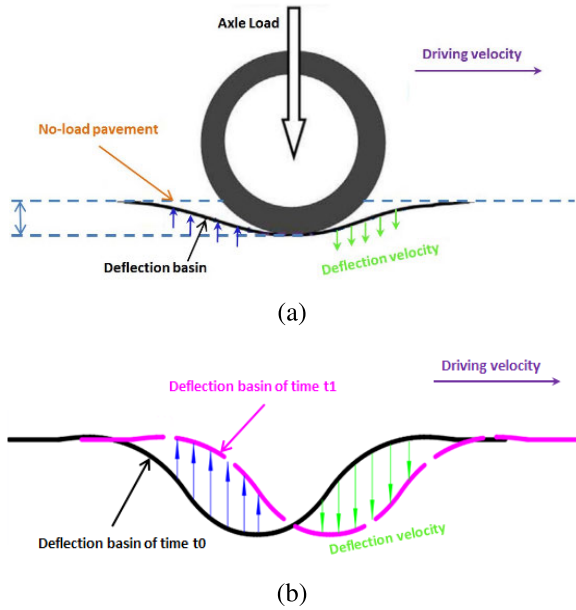


**FIGURE 1.** Principle of dynamic deflection measurement:(a) Pavement deflection; (b) Dynamic deflection basin.

disturbance that propagates through a material, causing deformation of the material around the dynamic deflection basin.

We consider the case of a massless Euler-Bernoulli beam of infinite length resting upon an elastic foundation of modulus  $k$ . The deflection  $d(x)$  under the force of a load  $F$  is estimated by the following expression [14]–[17]:

$$\begin{cases} d(x) = -\frac{1}{2} \cdot \frac{A}{B} \cdot e^{-Bx} \cdot (\cos(Bx) + \sin(Bx)) \\ A = \frac{F}{\sqrt{4EI k}}, \quad B = \left(\frac{k}{4EI}\right)^{1/4} \end{cases} \quad (1)$$

where  $x$  is the position of the deflection basin, and the force  $F$  is located at  $x = 0$ .  $E$  is the pavement rigidity modulus, and  $I$  is the pavement moment of inertia. Once the values of  $A$  and  $B$  are obtained, the deflection at any position on the deflection curve can be calculated.

For the derivatives on both sides of (1), the slope of the beam deflection curve at point  $x$  is:

$$d'(x) = e^{-Bx} \cdot A \sin(Bx) \quad (2)$$

where the rate of distance  $d'(x)$  is equivalent to the rate of vertical slope  $\Delta S_v(x)$  divided by the rate of horizontal slope  $\Delta S_h(x)$  at any moment, and is also equivalent to the ratio of the vertical deformation velocity  $V_r$  to the horizontal velocity  $V_h$  at any moment.

$$d'(x) = \frac{\Delta S_v(x)}{\Delta S_h(x)} = \frac{V_r(x)}{V_h(x)} \quad (3)$$

Parameters  $A$  and  $B$  can be estimated by

$$\begin{cases} e^{-Bx_1} \cdot A \sin(Bx_1) - V_{r1}/V_{h1} = 0 \\ e^{-Bx_2} \cdot A \sin(Bx_2) - V_{r2}/V_{h2} = 0 \\ \dots \\ e^{-Bx_n} \cdot A \sin(Bx_n) - V_{rn}/V_{hn} = 0 \end{cases} \quad (4)$$

**FIGURE 2.** The laser dynamic deflectometer. (a) The method of continuous dynamic deflection measurement. (b) The vehicle measuring system of the laser dynamic deflectometer.

where more than two validation points ( $x_1, x_2 \dots x_n$ ) are given, a Newton iterative algorithm would be used for the estimation of these parameters, and then the maximum deflection value of the load center ( $x = 0$ ) can be obtained by  $d(0) = -\frac{A}{2B}$ .

### B. THE LASER DYNAMIC DEFLECTOMETER

Based on the above principle, the LDD achieves velocity-based continuous pavement deflection measurement. Figure 2a shows that the LDD exerts a standard vehicle load to the center position of the pavement surface. More than four laser Doppler vibration meters are mounted on the measuring beam and measure the pavement deformation velocity caused by the action of the load wheel. A vehicle measuring system is integrated for effective and continuous measurement (as shown in Figure 2b). The related equipment and the supporting environment are installed in a container-size unit on a trailer.

The points with a larger deformation velocity are selected for precise measurement. The extreme value of deformation velocity  $y''(x)$  is obtained by

$$y''(x) = AB[\cos(Bx) - \sin(Bx)]e^{-Bx} = 0 \quad (5)$$

By solving the equation  $x = (n\pi + \pi/4)/B$ , it was found that the maximum slope is the one nearest to the load center  $x = \pi/(4B)$ . According to the Chinese High Grade Road Construction Standard, the pavement deflection basin radius should be within 3.5 m [14]. Three Doppler laser sensors  $S_i$  ( $i = 1, 2, 3$ ) are used to measure the velocities  $V_{di}$  at different positions ( $x_{i=1} = 100$  mm,  $x_{i=2} = 300$  mm, and  $x_{i=3} = 750$  mm away from the loading center). The velocities of the Doppler laser sensors  $V_{di}$  can be divided into the component of the horizontal velocity of beam  $V_h$ , the vibration velocity of beam  $V_v$ , the rotation velocity of beam  $V_{\omega i}$ , and the deflection velocity of road pavement  $V_{ri}$ . A Doppler laser sensor ( $S_4$ ) is installed 3,600 mm away from the center to measure the velocity outside of the basin ( $V_{d4}$ ). This velocity of the Doppler laser sensor  $V_{d4}$  is outside of the deflection basin and does not include the pavement deformation velocity of road pavement  $V_{ri}$ . Each sensor maintains a certain angle  $\alpha_i(2-2.5^\circ)$  against the measuring beam. Considering that the angle between the measuring beam and pavement surface is  $\theta$ , the velocity of each Doppler laser sensor is:

$$V_{di} = V_h \sin(\alpha_i + \theta) + V_v \cos(\alpha_i + \theta) + V_{\omega i} \cos(\alpha_i) + V_{ri} \cos(\alpha_i + \theta) \quad (6)$$

where the pavement deformation velocity outside the deflection basin is 0, and the distance from the sensor to the center of rotation axis  $l_i$  is:

$$V_{\omega i} = \frac{l_i G_x \pi}{180} \quad (7)$$

where  $G_x$  is the angular velocity of the measuring beam, as measured by gyroscope.

Both angles of the measuring beam  $\alpha_i$  and  $\alpha_i + \theta$ , are less than  $5^\circ$ , so the values of  $\cos(\alpha_i)$  and  $\cos(\alpha_i + \theta)$  are approximately equal to 1. The velocity of each Doppler laser sensor is simplified as

$$V_{di} = V_h \sin(\alpha_i + \theta) + V_v + V_{\omega i} + V_{ri} \quad (8)$$

The angle between the measuring beam and the pavement (with reference to the data of the Doppler vibrometer) is:

$$\theta = \arcsin\left(\frac{V_{d4} - V_v - V_{\omega 4}}{V_h}\right) - \alpha_4 \quad (9)$$

By combining (8) and (9), the pavement deflection velocity is

$$V_{ri} = V_{di} - V_v - V_h \sin[(\alpha_i - \alpha_4) + \arcsin\left(\frac{V_{d4} - V_v - V_{\omega 4}}{V_h}\right)] - V_{\omega i} \quad (10)$$

where high-precision up-down vibration velocity is difficult to obtain directly. Therefore, it is necessary to consider the influence of the vertical vibration velocity of the measuring beam. Equation (10) can be rewritten as:

$$V_{ri} = V_{di} - (V_{d4} - V_{\omega 4}) \cos(\alpha_i - \alpha_4) - V_{\omega i} - V_h \sin(\alpha_i - \alpha_4) \cos\left[\arcsin\left(\frac{V_{d4} - V_{\omega 4}}{V_h}\right)\right] + \varepsilon_1 \quad (11)$$

by defining  $\varepsilon_1$  as:

$$\begin{aligned} \varepsilon_1 = & -V_v(1 - \cos(\alpha_i - \alpha_4)) + V_h \sin(\alpha_i - \alpha_4) \\ & \cdot \{\cos[\arcsin\left(\frac{V_{d4} - V_{\omega 4}}{V_h}\right)] \\ & - \cos[\arcsin\left(\frac{V_{d4} - V_v - V_{\omega 4}}{V_h}\right)]\} \end{aligned} \quad (12)$$

In theory and practice, in the circumstance of a horizontal velocity of  $V_h = 72$  km/h,  $V_{d4}$  is about 700 mm/s,  $V_{\omega 4}$  is  $\pm 100$  mm/s, and  $V_v$  is  $\pm 450$  mm/s. As a result, the maximum absolute value of  $\varepsilon_1$  is 0.06 mm/s. The pavement deformation velocity is small, and the influence of the vertical vibration velocity of the beam on the measurement results can be ignored [14]. Equation (11) can thus be rewritten as:

$$V_{ri} = V_{di} - V_{d4} \cos(\alpha_i - \alpha_4) - \frac{G_x \pi}{180}(l_i - l_4) - V_h \sin(\alpha_i - \alpha_4) + \varepsilon_2 \quad (13)$$

by defining  $\varepsilon_2$  as:

$$\varepsilon_2 = V_{\omega 4}(\cos(\alpha_i - \alpha_4) - 1) + V_h \sin(\alpha_i - \alpha_4) \cdot [1 - \cos(\arcsin\left(\frac{V_{d4} - V_{\omega 4}}{V_h}\right))] \quad (14)$$

Similarly, the maximum absolute value of  $\varepsilon_2$  is 0.04 mm/s. It is considered that, as the influence of the rotating center of the beam on the pavement deformation velocity is ignored,  $(l_i - l_r)$  is related to the relative position of the sensor installation, so the deformation velocity of the pavement is

$$V_{ri} = V_{di} - V_{d4} \cos(\alpha_i - \alpha_4) - V_h \sin(\alpha_i - \alpha_4) - \frac{G_x \pi}{180}(l_i - l_4), \quad i = 1, 2, 3 \quad (15)$$

When the installation angle difference between the sensor is given, the pavement deformation velocity of the measured point can be calculated by combining the measured values of the sensor, gyroscope, and encoder.

### C. CALIBRATION METHOD

Equation (15) shows that the installation angle of the Doppler sensor will directly affect the accuracy of the pavement deformation velocity extraction. The difference of the sensor installation angle ( $\alpha_i - \alpha_4$ ,  $i = 1, 2, 3$ ) between inside and outside of deflection basin is normally  $\pm 0.2^\circ$ . Considering a vehicle speed of 70 km/s, the measurement error caused by the horizontal movement speed is  $\pm 70$  mm/s, while the component of the pavement deformation velocity is 2–40 mm/s. Thus, a calibration strategy should be presented to build multiple measurement equations and calculate the system parameters for the deflection measurement.

In the calibration of an LDD [22], the velocity sensor is installed at an angle  $\alpha_i$  (as shown in Figure 3), and the measuring beam and the baffle are statically placed at an angle  $\theta$  ( $-2^\circ \leq \theta \leq 2^\circ$ ). The smooth baffle, with a high-precision distance sensor, slides on the sliding track. The sliding of the baffle  $V_b$  is numerically equal to the horizontal velocity of beam  $V_h$ , and the partial velocity of Doppler sensor  $V_{di}$  is

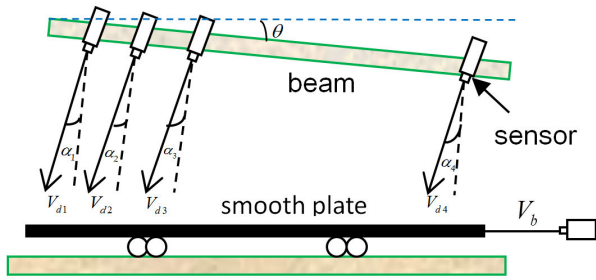


FIGURE 3. Calibration method for the continuous dynamic deflectometer.

given by the sliding direction of the baffle, to monitor the distance between the baffle and the measurement device in real time. In this case, the system is governed by

$$V_{di} = V_h \sin(\alpha_i + \theta) \quad i = 1, 2, 3, 4 \quad (16)$$

where both  $\theta$  and  $\alpha_i$  are small, and the velocity difference between the first three sensors and the fourth sensor satisfies

$$V_{di} - V_{d4} = V_h \sin(\alpha_i - \alpha_4) \quad i = 1, 2, 3 \quad (17)$$

When combined with the least-squares estimation method, the installation angle of sensor  $\alpha_i$  and the difference between sensors  $\alpha_i - \alpha_4$  can be obtained.

### III. CORRECTION MODEL FOR THE CONTINUOUS DYNAMIC DEFLECTOMETER

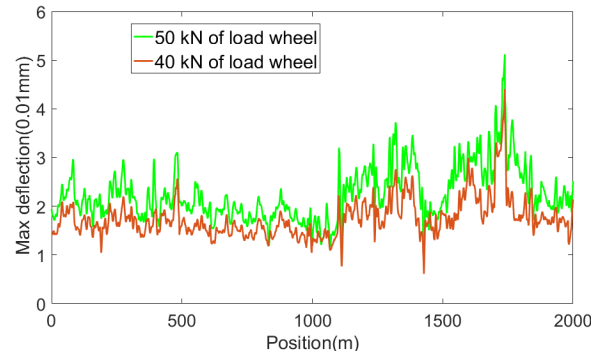
Continuous dynamic deflectometers have been widely developed in recent years, and have been applied experimentally in some countries. It has been found that these deflectometers are influenced by many factors, e.g., wheel load, vehicle speed, pavement roughness, and pavement temperature. There has been much research on static deflectometers, but few studies have considered the correction of continuous dynamic deflectometers.

#### A. INFLUENCING FACTOR ANALYSIS

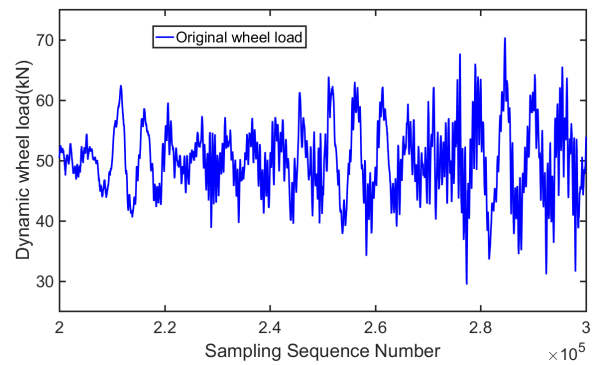
##### 1) DYNAMIC LOAD

An asphalt pavement will deform under the action of the load when the wheel passes, and then the measured result of the deflection value is obtained from the inversion of the deformation velocity. A given pavement can only be in one deflection value at any moment; however, different measurement results can be obtained under different conditions, e.g., pavement temperature and vehicle speed. This is a contradiction that needs to be corrected in the calculation process of the dynamic deflection measurement.

Dynamic load is the direct factor affecting pavement deformation. The larger the load, the greater the deformation velocity, and the larger the calculated deflection value. Figure 4a shows the deflection values calculated directly from (4) and (6), where the green line is the measured value for 100 kN (two wheels, each of 50 kN) and the red line is the measured value for 80 kN (two wheels, each of 40 kN).



(a)



(b)

FIGURE 4. Dynamic wheel loading of a continuous dynamic deflectometer. (a) Measured results under different standard loads. (b) Dynamic load in the measuring process.

It can be seen that the different wheel loads lead to different measured results. A change of vehicle attitude and pavement condition, such as roughness, will lead to a change in the action of the wheel load, which makes the measured deflection value inconsistent with its actual value. Figure 4b shows a typical dynamic load on rough asphalt pavement, where the IRI of the tested pavement is about 4–5 and the vehicle speed is approximately 80 km/s. The data in the figure show that the dynamic wheel load changes as the vehicle travels, which does have an effect on the accuracy of the measured results.

##### 2) VEHICLE SPEED

Because the measured result of the deflection value is obtained from the inversion of the deformation velocity, both the vehicle speed and deformation velocity are components of the velocity value of the Doppler laser sensors. Usually, the combined velocity of the Doppler laser sensors is about 300–1300 mm/s, the component of the vehicle speed along the excitation line is 200–1100 mm/s, and the pavement deformation velocity is less than 40 mm/s. Thus, the influence of vehicle speed cannot be neglected. The effect of vehicle speed on the measured velocity of pavement deformation is given in (15), and the effect of the measured velocity on the deflection calculation and correction is given in (4).

### 3) PAVEMENT ROUGHNESS

Pavement roughness is defined as a manifestation of the pavement surface smoothness, which is usually evaluated by the IRI. Reports have shown that pavement roughness has a great influence on the TSD [21]. The traveling vibration changes the attitude of the measuring vehicle and leads to changes in the wheel load and changes of the measuring beam attitude, especially for pavement with an IRI of greater than 3. Figure 4a shows the effect of changes in the wheel load. For the effect of changes in the measuring beam attitude, the LDD measuring beam is rigidly connected with the Doppler laser sensors (as shown in Figure 3), and the velocity component produced by the beam attitude is a component of the sensor measurement result. For the separation of pavement deformation velocity, this component is a large noise signal, which should be taken into account in the measurement and calculation. Equation (15) uses the gyroscope to acquire the real-time attitude of the measuring beam, eliminating the velocity component caused by the attitude change of the sensor. Through the correction of the velocity component of the gyroscope, there will only be a tiny error in calculating the deflection value.

### 4) PAVEMENT TEMPERATURE

Pavement temperature is the primary influencing factor of pavement bearing capacity [19], [23]–[30], especially for asphalt pavement. Surface pavement temperature can vary widely over the course of a day, and may approach 70°C during the summer period. From the material characteristics, moisture will affect the cohesion of the subgrade, and the thickness of the pavement layer can reflect the pavement cohesion. The measured values at a high temperature are usually larger than those taken at a low temperature. Pavement temperature correction is widely recognized as being a difficult problem, and debate continues about the best strategy for the temperature modification models. Normally, the influence of pavement temperature on the measured deflection value is corrected by a temperature correction coefficient, such as the following

$$D_{T_{ref}} = D_T K_T \tag{18}$$

where  $D_{T_{ref}}$  is the reference deflection value at reference temperature  $T_{ref}$ ,  $D_T$  is the actual measured result of the deflection value, and  $K_T$  is the temperature correction coefficient at the actual temperature  $T$ . The different correction coefficients are shown in Table 1.

The temperature correction coefficient  $K_T$  is assumed to depend on many factors, such as the actual temperature  $T$ , total asphalt thickness  $H$ , the modulus of resilience  $E_0$ , cracking state  $C$ , location of measurement points in lanes  $L$ , type of subgrade  $S$ , and subgrade material  $M$ . The main influencing factors of the temperature correction coefficient (actual temperature and total asphalt thickness) are identical; however, deviations exist in the other factors.

The use of continuous dynamic deflectometers is on the rise in recent years, but few studies have investigated the

**TABLE 1. Correction of the temperature effect on a continuous dynamic deflectometer.**

Author	Depends on factors	$T_{ref}$	Relationship
AASHTO [19]	$T, H, M$	21.1°C	Graph/nomograph
MOT [26]	$T, H, E_0$	20.0°C	Equation
SHRP [27]	$T, H, S$	21.1°C	Graph/nomograph
Zheng et al. [28]	$T, H$	20.0°C	Equation
Chen et al. [29]	$T, H, C, T_{ref}$	-	Equation
Kim et al. [30]	$T, H, L$	20.0°C	Equation

temperature correction of continuous dynamic deflectometers in a systematic way. Using curviameter equipment, García and Castro undertook deflection testing at different temperatures and the same vehicle speed (about 5 m/s) during the same day [20]. However, because of the lack of experimental samples, the conclusions of this study were limited to pavements composed of 250 mm of asphalt mix and an asphalt temperature of 15–25°C. The Texas Department of Transportation has reported that it would be more practical to establish the temperature correction relationship using a device with more than three sensors [31].

### 5) OTHER INFLUENCING FACTORS

Subgrade humidity, pavement thickness, and the type of pavement structure also have an influence on the propagation of the deflection wave. However, there is no sensor for these attributes that can quickly and accurately obtain the parameter information. Therefore, these factors are not discussed in this article.

In summary, in the range of measurement conditions, the influence of the dynamic wheel load, vehicle speed, and pavement temperature are considered in the correction processing of the continuous dynamic deflectometer.

## B. ESSENTIAL DATA FOR THE CORRECTION MODEL

For the dynamic deflection, its measured value and actual value (reference value) are different, so we need to establish a modified model in order to correct the influencing factors. However, at present, there is no internationally recognized continuous dynamic deflectometer that can be used to make a comparison. For reference, the measurement values of the BBD and FWD are selected in this article. Both of the BBD and the FWD are based on the measurement of static, low-speed, and non-continuous sampling, for which the sampling interval is 10–50 m.

A sample of the selected deflection correction data is shown in Figure 5. By combining the installation parameters of the Doppler sensor obtained by the calibration method, the pavement deformation velocity extracted by (15), and the slope equation of the deflection basin in (4), the deflection value was calculated by the Newton iteration method. The correction data for the dynamic deflection measurement were derived from the actual traffic pavement. The axle loads were obtained by strain gauges or accelerometers installed on the

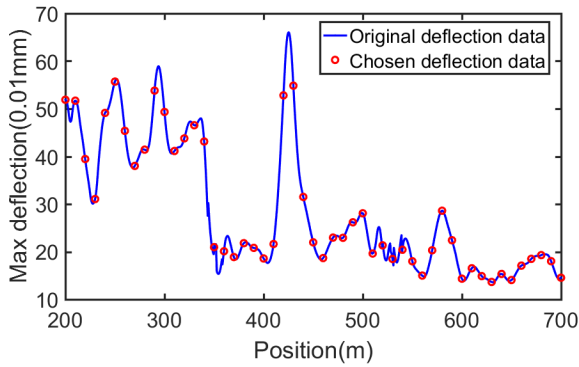


FIGURE 5. Selection of deflection values to be corrected based on registration points.

load wheels, pavement temperature was measured directly by temperature sensors, and vehicle speed was converted from the distance encoders. To ensure that the data involved in the calculation of the correction model covered as much as possible, different pavement conditions, different vehicle speeds, and different surface temperatures were considered. In addition, the measured points with a large difference between the reference value and LDD value were removed, to prevent system error and reference measurement error in the regression.

Figure 6 the data used to establish the correction model. These data were chosen from different measurement sections and conditions. The red line in Figure 6a the reference deflection value measured by the BBD or FWD, and the blue line is the dynamic deflection value of the LDD. The reference value and the dynamic deflection value show synchronous changes at the registration points, and the difference between them (orange line) is relatively stable. Figure 6b and Figure 6c respectively give vehicle speeds and pavement temperatures, which satisfy the general continuous deflection measurement conditions. The former ranges from 5 m/s to 23 m/s (18 km/h to 82.8 km/h), and the latter ranges from 7°C to 42°C. The rolling loads of the equipment (shown in Figure 6d) were recorded by strain gauges.

C. THE CORRECTION MODEL FOR THE DYNAMIC DEFLECTION VALUES

A correction coefficient is a general method that can be used in dynamic deflection measurement. Here, the deflection correction is assumed as being

$$Y_M = Y_O F \tag{19}$$

where  $Y_O$  is the measured value of the pavement deformation,  $Y_M$  is the corrected value of the pavement deflection, and  $F$  is the comprehensive correction coefficient of the multiple influencing factors. The corrected value depends on the linearity of multiplication by the measured value.

By using a regression analysis method, a comprehensive correction relationship between the revised coefficient  $F$  and the influencing factors (pavement temperature, vehicle speed,

and dynamic load) is established. The relationship between the factors and the target is unknown, so the basic quadratic regression model of the three variables is established as follows

$$F = b_0 + \sum_{k=1}^3 b_k X_k + \sum_{k=1}^3 \sum_{p=k}^3 b_{kp} X_k X_p + \epsilon \tag{20}$$

$$\min \epsilon^2 = \min \sum_{i=1}^n [F - (b_0 + \sum_{k=1}^3 b_k X_{ki}) + \sum_{k=1}^3 \sum_{p=k}^3 b_{kp} X_{ki} X_{pi}]^2 \tag{21}$$

where  $b$  is the regression coefficient;  $X$  is the influencing factor;  $\epsilon$  is the error term, which obeys a standard normal distribution. The subscripts correspond to the different influencing factors, where there are three factors to be considered:  $k = 1$  or  $p = 1$  correspond to the vehicle speed;  $k = 2$  or  $p = 2$  correspond to the dynamic load; and  $k = 3$  or  $p = 3$  correspond to the pavement temperature. Considering a total number  $n$  of observation samples, the minimum variance satisfies (21).

Equation (19) shows that  $F$  is equal to the corrected deflection value, rather than the actual measured original deflection value  $F = Y_M/Y_O$ . In the process of revision,  $Y_M$  takes the corresponding measurement points of the BBD or FWD in the regression analysis. By expanding the regression model, nine regression terms with influencing factors can be obtained. These regression terms are  $X_1, X_2, X_3, X_1X_2, X_1X_3, X_2X_3, X_1^2, X_2^2$  and  $X_3^2$ . Although the relationship between the factors and objectives is unknown, fewer regression terms are preferred to describe the model. Table 2 gives the statistical results for different numbers of regression terms, where the optimum regression model and its parameters for the different regression terms are marked in bold.

The best correlation for the regression results is 0.62285 for the condition of one influencing term, but the results of the regression correlation, root-mean-square error, and mean absolute error are poor. The correlation, root-mean-square error, and mean absolute error of the regression results are significantly improved for the condition of two influencing terms. The best result is obtained for the condition of three influencing terms, where the difference between the regression result and the best regression correlation coefficient, root-mean-square error, and average absolute error is small, and the best  $F$  statistic value is achieved. For the condition of more than three influencing terms, the regression correlation coefficient increases slightly with the increase of the number of factors, but the  $F$  statistic value decreases. The larger the number of influencing terms, the more complex the regression model is. The overall performance is the best when three influencing terms are used, and the corresponding regression model is thus recommended.

Table 3 lists the real influencing terms used in the best regression model with different numbers of

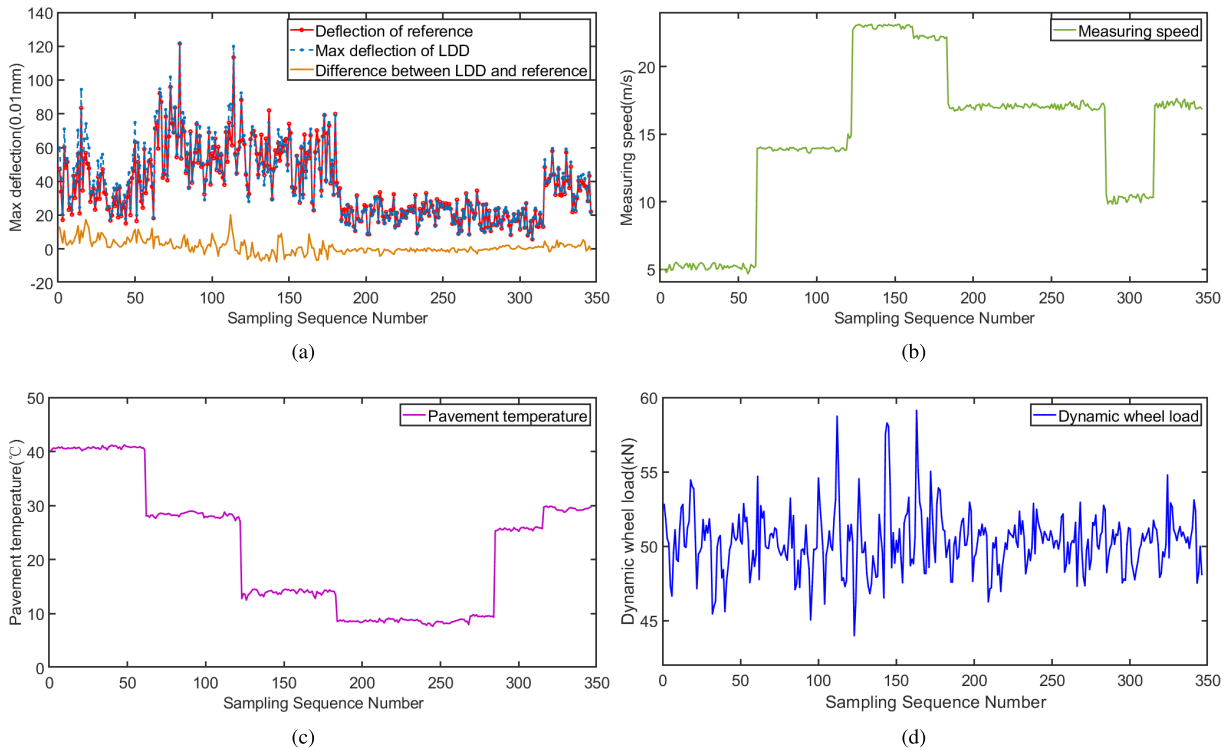


FIGURE 6. Data for the correction model: (a) deflection value; (b) vehicle speed; (c) pavement temperature; (d) dynamic wheel load.

TABLE 2. Statistical parameters of the regression model.

Num <sup>a</sup>	Correlation coefficient	Statistics coefficient, <i>F</i>	Average absolute error	RMSE
1	0.62285	568.1	0.04112	0.051323
2	0.91416	1826.4	0.018735	0.024485
3	<b>0.94541</b>	<b>1974.1</b>	<b>0.015015</b>	<b>0.019527</b>
4	0.94678	1516.7	0.014672	0.019279
5	0.94744	1225.7	0.01455	0.01916
6	0.94781	1026.1	0.014471	0.019092
7	0.9482	883.8	0.014392	0.019021
8	0.94824	771.69	0.014358	0.019014
9	0.94835	685.54	0.014369	0.018992

<sup>a</sup> Numbers of regression terms  
The overall model was significant at the 0.01 level with an F statistic

influencing factors. “√” indicates that the corresponding influencing terms are valid in the model, whereas “×” means

TABLE 3. Influencing factors used in the regression model.

Numbers of influencing factors	Influencing terms										Primitive factors
	$X_1$	$X_2$	$X_3$	$X_1X_2$	$X_1X_3$	$X_2X_3$	$X_1^2$	$X_2^2$	$X_3^2$		
1	×	×	×	×	×	√	×	×	×	$X_2, X_3$	
2	×	√	×	×	×	×	×	×	√	$X_2, X_3$	
3	√	√	√	×	×	×	×	×	×	$X_1, X_2, X_3$	
4	√	√	√	×	×	×	×	√	×	$X_1, X_2, X_3$	
5	√	√	√	×	×	×	×	√	√	$X_1, X_2, X_3$	
6	√	√	×	×	√	×	√	√	√	$X_1, X_2, X_3$	
7	√	√	√	×	√	×	√	√	√	$X_1, X_2, X_3$	
8	√	√	√	√	√	×	√	√	√	$X_1, X_2, X_3$	
9	√	√	√	√	√	√	√	√	√	$X_1, X_2, X_3$	

that the corresponding influencing terms are invalid in the model. For the condition of one influencing term,  $X_2X_3$  is the best regression model. For the condition of two influencing terms,  $X_2$  and  $X_3^2$  are the best regression models, and so on.

Compared with the original influencing term (vehicle speed), the influencing terms of dynamic load and pavement temperature have an obvious influence on the direct measurement of the continuous deflection. Thus, a recommended correction model is given as follows:

$$F = 2.1813 + 0.00597X_1 - 0.02431X_2 - 0.0032X_3 \quad (22)$$

The vehicle speed is positively correlated with the correction coefficient (the higher the vehicle speed, the larger the correction coefficient); there is negative correlation between the dynamic load and the correction coefficient (the larger



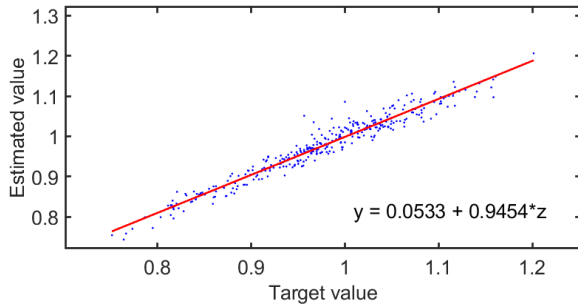


FIGURE 7. Correction function of the deflection value.

the dynamic load, the smaller the correction coefficient); and there is negative correlation between the pavement temperature and the correction coefficient (the higher the pavement temperature, the smaller the correction coefficient). The original deflection measured by the LDD is corrected according to (21). The corrected results are shown in Figure 7, where the blue points are the original data and the red line is the fitting result. The horizontal axis is the target value of the regression analysis, and the vertical axis is the expected value of the regression analysis.

The difference (mean absolute error: 0.52; maximum absolute error: 2.89) between the corrected LDD deflection value and the reference value is significantly smaller than that of the LDD deflection value before correction (mean absolute error: 2.87; maximum absolute error: 20.20). The correlation between the corrected LDD deflection value and the reference value (0.9995) is also higher than that of the LDD deflection value before correction (0.983). Better correction results are obtained under the condition of simultaneously correcting the influence of dynamic load, pavement temperature, and vehicle speed. Figure 8 shows the comparison of before and after correction.

The red line in Figure 8a is the reference deflection value, and the blue line is the corrected deflection of the LDD. The difference between them is represented by the green line in Figure 8b, and the orange line is the difference between the actual measured value and the reference value before correction. Here, the BBD and FWD values were selected as the reference values.

IV. EXPERIMENTS

Experiments were conducted to verify the environmental adaptability and system reliability of the continuous dynamic deflectometer and the recommended correction method. The repeatability index and correlation index were selected to verify the robustness of the continuous dynamic deflectometer under various potential influencing factors. Repeatability is used to measure the stability of the system, in that a good measurement method has good repeatability. Correlation is used to evaluate the consistency (accuracy) of the results among different devices. The guidelines for the experiments are shown in Table 4.

The experiments were divided into two parts: repeatability experiments and correlation experiments. The calculation

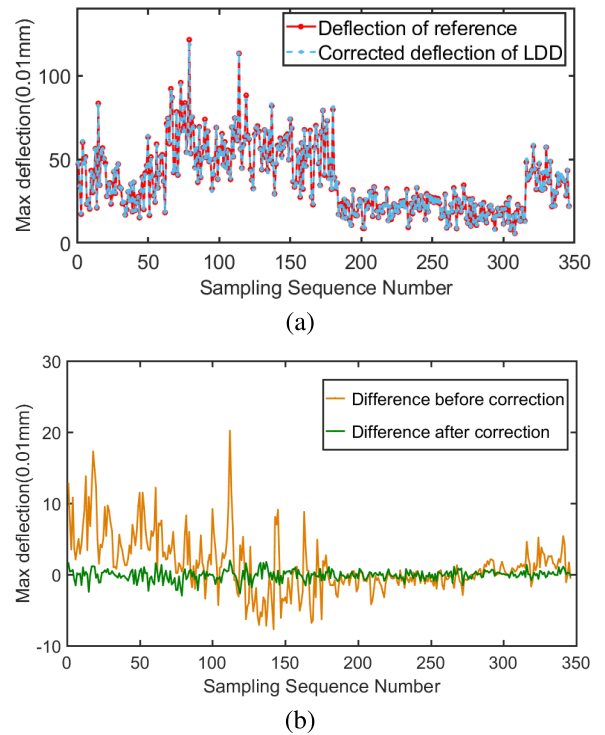


FIGURE 8. Comparison of deflection values before and after correction: (a) correction of the deflection value; (b) errors before and after correction.

TABLE 4. Experimental requirements.

Categories	Experimental condition
Repeatability	Different vehicle speeds: 20–80 km/h
	Different pavement roughness: IRI>6
	Different pavement structure: Composite/flexible
	Different pavement temperature: 0–45°C
Correlation	LDD and FWD: Different pavement roughness
	LDD and FWD: Different vehicle speeds
	LDD and BBD: Different pavement structure
	LDD and BBD: Different pavement temperature
Between LDDs	Same condition

methods for repeatability  $P$  and correlation  $R$  are

$$P_X = (1 - \sqrt{\sum_{j=1}^n (X_j - \bar{X})^2 / (n - 1) / \bar{X}}) \times 100\% \quad (23)$$

$$C_X = 1 - P_X \quad (24)$$

$$R_{XY} = \sum_{i=1}^n \frac{(X_i - \bar{X})(Y_i - \bar{Y})}{\sqrt{\sum_{j=1}^n (X_j - \bar{X})^2 \cdot \sum_{j=1}^n (Y_j - \bar{Y})^2}} \quad (25)$$

where  $P_X$  is the repeatability of sample  $X$ ;  $X_i, Y_i$  is the measurement value of sample  $i$ ;  $\bar{X}, \bar{Y}$  is the mean of the sample;  $C_X$  is the deviation coefficient of sample  $X$ ; and  $R_{XY}$  is the correlation coefficient between sample  $X$  and sample  $Y$ .

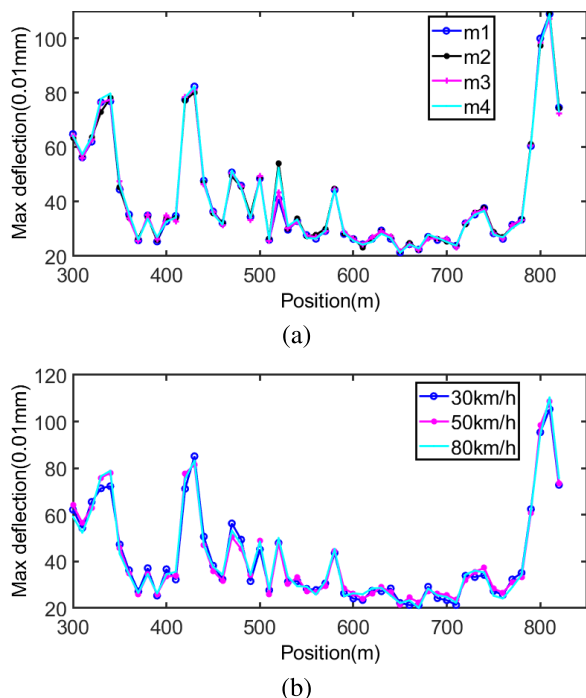


**FIGURE 9.** Effect of speed on the repeatability of the detection: (a) repeatability at the same vehicle speed; (b) repeatability at different vehicle speeds.

**A. REPEATABILITY OF THE MEASUREMENT RESULTS**

The repeatability coefficient is a value representing the absolute difference between two repeated results, which can be expected to lie as a probability. The repeatability is widely used as an evaluation indicator for the working reliability of a measurement system.

**1) DIFFERENT VEHICLE SPEEDS**

To verify the influence of vehicle speed, two sets of LDD measurements were utilized, both recorded at a driving speed of 20–90 km/h. Figure 9a is the result of the repeated measurements at the same speed, showing the results of four measurements, respectively (m1, m2, m3, and m4). The symbols are the same in both figures. Figure 9b is the result of the repeated measurements at different vehicle speeds.

It can be seen from Table 5 that the repeatability of the measured results (m5, m6 and m7 are measured at 30 km/h, 50 km/h and 80 km/h respectively) is more than 98%, and the deviation caused by vehicle speed is less than 5% under different times and speeds (30–80 km/h). The results show that accurate measurement results are obtained by the proposed method, with good repeatability, and the results are only slightly influenced by the vehicle speed.

**2) DIFFERENT PAVEMENT ROUGHNESS**

A change of pavement roughness affects vehicle attitude and wheel load, especially for pavement with an IRI of greater than 3. The LDD uses a gyroscope to acquire the real-time

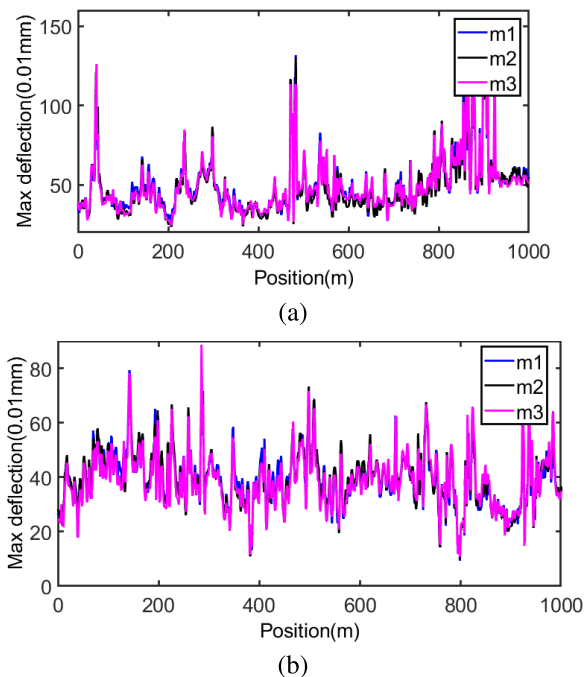


**FIGURE 10.** The effect of roughness on measurement repeatability: (a) pavement section A (IRI = 6.5); (b) pavement section B (IRI = 8.3).

measuring beam attitude, to eliminate the velocity component caused by the vehicle attitude. The potential impact of pavement roughness on the measurement is mainly reflected in the high frequency of the dynamic load (because the IRI uses an interval evaluation method, the smallest evaluation unit is 10 m, and the frequency of pavement load change is high, it is impossible to directly replace the influencing factor of dynamic load by pavement roughness). In this article, we indirectly verify the measurement results under different dynamic loads through the consistency of the measurement results of different pavements.

Dozens of pavements with different IRI values were tested, and two representative pavement sections are depicted in Figure 10, which shows the results of repeated measurements in the same pavement sections. Both pavement sections (Figure 10a and Figure 10b) featured poor roughness of the asphalt pavement surface. Each pavement section was 1 km in length, and was measured three times.

The average repeatability of the two pavement sections is 95.5% and 95.7%. It can therefore be concluded that the roughness of the pavement has little influence on the repeatability of LDD measurements. This is despite the fact that the undulation of the pavement surface affects the instantaneous load exerted by the load wheel on the pavement surface, resulting in a larger rotation attitude of the measuring beam. The real-time attitude of the measuring beam is derived by a mathematical model of the system, and the dynamic load of the influencing factors is corrected by the proposed correction model.

TABLE 5. The repeatability at different vehicle speeds (unit of m1–m7: 0.01 mm).

Position (m)	Repeated experiment at 50 km/h					Effect of vehicle speed			
	m1	m2	m3	m4	$P_x$	m5	m6	m7	Deviation
300	64.8	63.5	64.3	64.2	99.1%	62.2	64.2	59.2	4.0%
320	62.0	63.5	62.8	63.8	98.8%	65.5	63.0	62.4	2.6%
340	76.8	78.0	77.4	79.7	98.4%	72.3	78.0	78.9	4.7%
360	35.3	34.2	33.8	35.7	97.4%	36.3	34.8	34.5	2.8%
380	35.0	34.1	35.2	33.7	98.0%	37.1	34.5	34.7	4.2%
400	32.7	33.8	34.9	32.7	96.9%	36.7	33.5	34.5	4.7%
420	77.4	77.1	78.3	78.3	99.2%	71.2	77.8	75.4	4.5%
440	47.7	47.0	46.4	47.4	98.8%	50.7	47.1	46.9	4.4%
460	32.1	32.2	31.3	31.6	98.8%	32.3	31.8	34.3	4.1%
480	45.9	45.4	45.5	44.8	99.0%	49.4	45.4	47.4	4.2%
500	48.5	48.9	49.5	48.4	99.0%	45.2	48.8	48.6	4.3%
520	40.9	54.2	43.4	52.4	86.3%	48.0	47.7	50.1	2.7%
540	32.8	33.8	32.6	33.4	98.4%	31.5	33.2	29.4	6.1%
560	26.3	27.9	27.0	26.5	97.3%	27.8	26.9	25.8	3.7%
580	44.3	44.7	44.4	44.7	99.6%	43.7	44.5	45.4	2.0%
600	26.3	26.4	26.4	25.7	98.7%	24.1	26.2	26.4	4.9%
620	26.3	26.5	26.9	25.2	97.3%	27.4	26.2	28.5	4.1%
640	26.4	27.0	27.3	26.6	98.5%	28.5	26.8	25.4	5.8%
660	24.4	24.9	24.4	24.3	98.9%	21.3	24.5	23.3	6.9%
680	27.1	27.0	26.5	27.9	97.9%	29.2	27.1	28.4	3.6%
700	25.8	25.2	26.3	25.2	98.0%	23.4	25.6	24.8	4.7%
720	32.1	31.7	32.1	31.7	99.3%	33.9	31.9	34.4	4.0%
740	37.6	37.7	37.2	36.6	98.6%	34.2	37.3	35.3	4.4%
760	26.3	27.0	26.3	26.9	98.6%	25.6	26.6	24.1	5.0%
780	33.4	33.5	33.3	32.6	98.8%	35.1	33.2	34.3	2.8%
800	99.9	97.3	98.4	97.7	98.8%	95.4	98.3	94.5	2.1%
Average	41.9	42.4	42.0	42.2	98.0%	41.7	42.1	41.8	4.1%

3) DIFFERENT PAVEMENT STRUCTURES

A composite structure pavement (concrete pavement at the bottom of the pavement, asphalt pavement at the top) and a flexible structure pavement (asphalt pavement at both the bottom and the top) were selected to verify the repeatability of LDD measurements in different pavement structures. The results of three consecutive measurements are shown in Figure 11, respectively. The red line in Figure 11a is the standard deviation of the three consecutive measurements.

The repeatability for the composite pavement is 85% and the repeatability for the flexible pavement is 95%. The repeatability of the calculation is low because the deflection value of the composite pavement is small. However, the standard deviation of each measurement point is far less than the measured deflection value, so the measured value can be considered as reliable.

4) DIFFERENT PAVEMENT TEMPERATURES

According to the external working temperature of the system, this experiment was aimed at showing the effect of different pavement temperatures (0–45°C). To minimize the influence of pavement structural strength changes on the evaluation of the measurement results, the time interval should be as small as possible. Thus, a pavement section was selected to measure the deflection over the course of 24 hours in autumn at 15:00, 20:00, and 3:00 the next day. The results of three times measurement are shown in Figure 12 and Table 6.

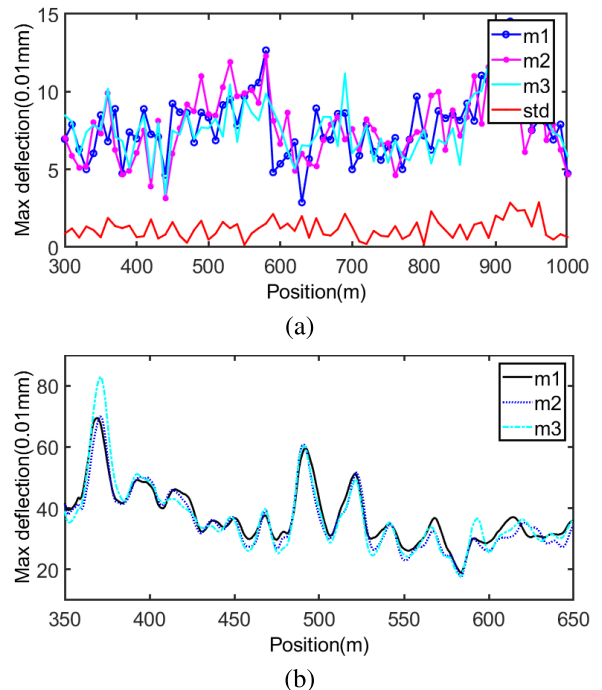
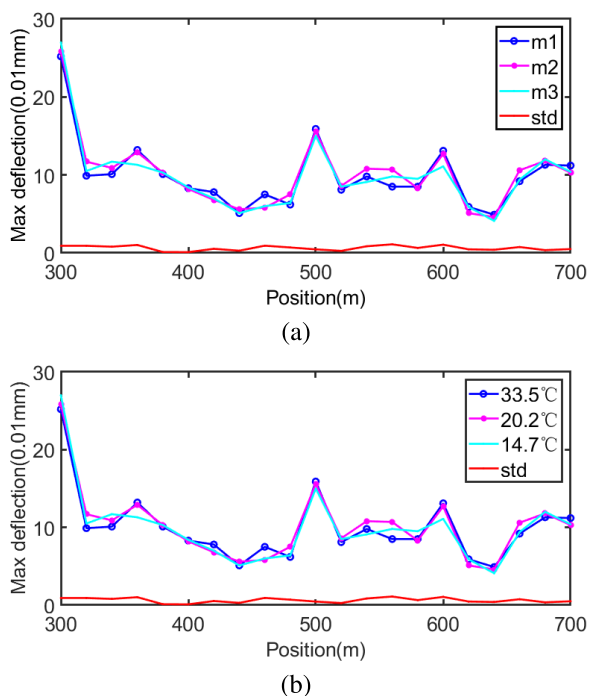


FIGURE 11. The effect of pavement structure on measurement repeatability: (a) composite structure pavement; (b) flexible structure pavement.

The red line in Figure 12 is the standard deviation of the three consecutive measurements. The deflection value for the composite pavement is small, and its repeatability is low.

**TABLE 6.** Measurement results under different temperatures (unit of m1–m3: 0.01 mm).

Position (m)	Pavement temperature 33.5°C				Pavement temperature 20.2°C				Pavement temperature 14.7°C			
	m1	m2	m3	$P_X$	m1	m2	m3	$P_X$	m1	m2	m3	$P_X$
300	25.2	25.8	27	96.5%	24.3	26.1	27.3	94.2%	25.4	25.1	27.4	95.2%
320	9.9	11.7	10.5	91.4%	10.2	11.4	11.3	93.9%	9.7	11.3	10	91.8%
340	10.1	10.9	11.7	92.7%	9.7	10.7	11.8	90.2%	10.3	10.2	11.6	92.7%
360	13.2	12.9	11.3	91.8%	12.5	13.4	10.7	88.7%	12.5	13.6	11.2	90.3%
380	10.1	10.3	10.3	98.9%	10.3	10.1	10.3	98.9%	9.7	10.7	10.3	95.1%
400	8.3	8.2	8.4	98.8%	8.5	7.7	8.3	94.9%	8	7.9	8	99.3%
420	7.8	6.8	7	92.7%	7.7	6.4	7.4	90.5%	8.1	6.6	7.5	89.8%
440	5.1	5.6	5.1	94.5%	6.2	5.8	4.9	88.2%	5.4	5.8	5.4	95.8%
460	7.5	5.8	6	85.6%	7.8	5.7	6.2	83.3%	7.7	6.5	7.3	91.5%
480	6.2	7.5	6.4	89.6%	5.4	5.4	5.5	98.9%	5.8	5.5	5.6	97.3%
500	15.9	15.6	15	97.0%	16.6	16	15.2	95.6%	16.8	15.3	15.2	94.3%
520	8.1	8.6	8.5	96.9%	7.9	9.5	8.4	90.5%	7.5	8.9	8.3	91.5%
540	9.8	10.8	9.1	91.4%	9.7	11	9.2	90.7%	9.2	10.6	8.5	88.7%
560	8.5	10.7	9.8	88.6%	8.7	10	10.1	91.9%	8.1	9.4	10.4	87.6%
580	8.5	8.3	9.5	92.7%	8.8	8.3	9	95.9%	8.2	9	8.9	95.0%
600	13.1	12.7	11.1	91.4%	13.2	12.6	10.5	88.3%	12.7	11.9	11.2	93.7%
620	5.9	5.1	5.9	91.8%	5.6	5.4	5.1	95.3%	5.5	5.6	5.8	97.3%
640	4.9	4.6	4.1	91.1%	5.3	4.7	4.5	91.4%	5.4	5.7	5	93.5%
660	9.2	10.6	9.4	92.2%	8.6	9.7	9.9	92.6%	7.5	8.3	9.3	89.2%
680	11.3	11.8	12	96.9%	11.2	12.2	12.4	94.6%	11.1	12.4	12.2	94.1%
700	11.2	10.3	10.4	95.4%	11.9	9.4	10.5	88.2%	12.8	10.8	11.3	91.1%
Average	9.99	10.22	9.93	93.2%	10.00	10.07	9.93	92.2%	9.88	10.05	10.02	93.1%



**FIGURE 12.** Effect of different pavement temperatures on the measurement results: (a) repeatability at the same temperature; (b) repeatability at different temperatures.

However, the standard deviation of each measurement point is far less than the measured deflection value, so the measured results can be considered as reliable, in this case. The deflection values for the different temperatures in Figure 12b are the average values of the measurements at the current temperature. After the temperature correction described in this article, the results of the measurements at different temperatures are

similar, which verifies the reliability of the proposed correction method.

**B. CORRELATION OF THE MEASUREMENT RESULTS**

The FWD, BBD and LDD are three typical deflectometers, with different measuring principles and mechanisms. As a result, the values measured directly by the different methods are different, as well as the shape and extremum of the pavement deflection. However, these methods all reflect the comprehensive bearing capacity of subgrade and pavement, so there should be a strong correlation between them. We compared the LDD with the FWD and BBD, and we also compared multiple LDDs. The measured results of the different devices were obtained within a 2-hour period, ensuring the consistency of the measurement environment.

**1) COMPARISON WITH A DYNAMIC IMPACT DEFLECTOMETER**

The FWD is a typical dynamic impact deflectometer, and its measurement interval is 10–50 m. It measures the total pavement deflection value under the action of the impact load. As a traditional reliable pavement deflectometer, the FWD is widely used in pavement deflection measurement.

To verify the accuracy of the measurement results, two pavement sections with different conditions were selected. A pavement with good roughness and a pavement with poor roughness were selected and tested. Three consecutive measurements were obtained at a vehicle speed of 50 km/h, and the average values of the LDD were compared with those of the FWD. Figure 13 shows the results of the measurements. AvgDef (blue line) is the average of the three consecutive measurements, and RefDef (red line) is the maximum

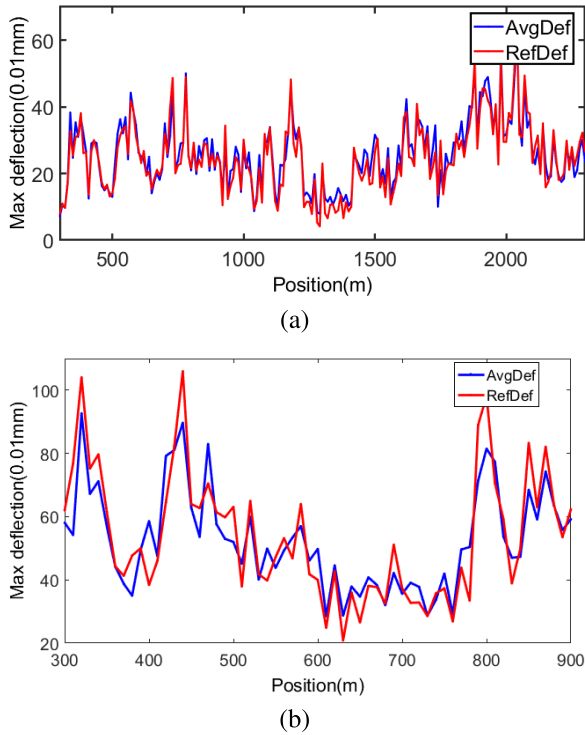


FIGURE 13. Correlation at different pavement roughness: (a) pavement A (IRI = 2.3); (b) pavement B (IRI = 7.2).

deflection measured. The correlation for Figure 13a and Figure 13b is 0.95 and 0.91, respectively. The results show that pavement roughness has little influence on the correlation between the FWD and the LDD, and the continuous dynamic deflectometer and the proposed correction method have good adaptability to different pavement roughness.

For each pavement section, velocities of 20 km/h, 45 km/h and 70 km/h were measured, and the correlation between the LDD and the FWD was then calculated. The results are shown in Table 7. The correlation at different speeds between the LDD and the FWD is about 0.95. Thus, it can be concluded that the vehicle speed has little influence on the correlation of the measurement.

2) COMPARISON WITH A STATIC DEFLECTOMETER

The BBD is a typical static deflectometer, and its measurement interval is 10–50 m. It measures the total pavement deflection value under the action of a static load. As a traditional reliable pavement deflectometer, the BBD is widely used in pavement deflection measurement, especially in developing countries. To verify the accuracy of the measurement results under different pavement structures and different pavement temperatures, the BBD deflection value was taken as a comparison.

A composite pavement and a flexible pavement were used to verify the effect of pavement structure. Three consecutive measurements were obtained at a speed of 50 km/h, and the results were compared with those of the BBD. Figure 14

TABLE 7. Correlation measurements at different velocities.

Position (m)	FWD (0.01 mm)	Effect of Speed (LDD)			Deviation
		20 km/h	45 km/h	70 km/h	
300	41.5	43.9	42.5	42.3	2.0%
310	50.1	44.8	44.4	45.8	1.6%
320	90.8	76.6	79	76.3	1.9%
330	55.8	47.5	49.4	50.2	2.8%
340	57.4	51	51.1	50.8	0.3%
350	64.6	51.7	50.5	49.6	2.1%
360	42.7	45.6	45.8	45.3	0.6%
370	51.6	45.7	44	43.7	2.4%
380	38.4	35.9	36.4	37.1	1.7%
390	30.4	37.4	37.2	36.7	1.0%
400	35.9	39.8	38.2	36.3	4.6%
410	28.2	31.3	32.9	36	7.2%
420	29.5	39.7	39.2	33.7	8.9%
430	32.7	33.2	36.9	38.8	7.8%
440	75.2	62.5	60.4	57.3	4.4%
450	35	43.1	39.3	37.9	6.7%
460	41.7	37.4	40	44.8	9.2%
470	53.5	52.4	46.8	42.4	10.6%
480	28.9	31.2	32	34	4.5%
490	35.5	37.3	36.1	34.7	3.6%
500	21.1	28.1	29.4	31.6	6.0%
Average correlation	–	0.96	0.96	0.95	–

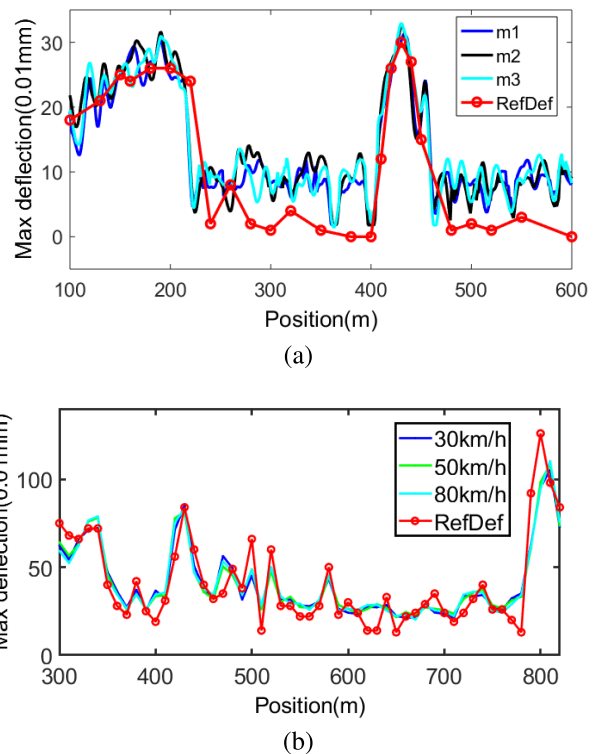


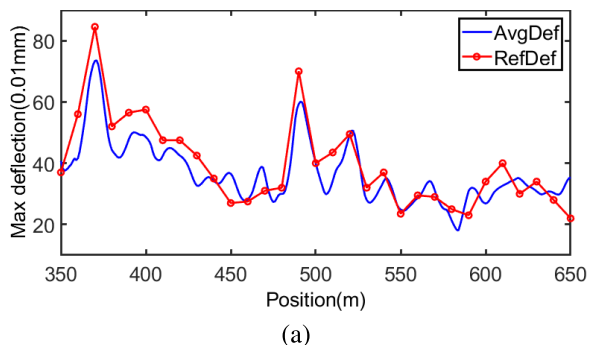
FIGURE 14. Correlation of the deflection measurement results in different pavement structures: (a) composite structure pavement; (b) flexible structure pavement.

shows the results, in which the correlation is 0.91 (composite pavement) and 0.92 (flexible pavement).

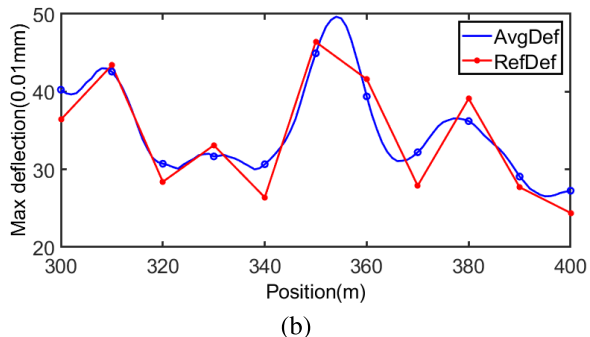
Two pavement sections with surface temperatures of 42°C and 13°C were used to verify the effect of pavement temperature. Three consecutive measurements were obtained at a speed of 50 km/h, and the results were compared with those of the BBD. Figure 15 shows the results of the

TABLE 8. Comparison of the continuous deflection measurement results.

	Autocorrelation of the individual LDD				Correlation of the multiple LDDs			
	$m_{11}$	$m_{12}$	$m_{13}$	$Avg_1$	$m_{21}$	$m_{22}$	$m_{23}$	$Avg_2$
$m_{11}$	1.000	0.984	0.987	0.995	0.982	0.979	0.995	0.990
$m_{12}$	-	1.000	0.984	0.994	0.982	0.977	0.987	0.987
$m_{13}$	-	-	1.000	0.995	0.983	0.977	0.989	0.988
$Avg_1$	-	-	-	1.000	0.987	0.983	0.996	0.993



(a)



(b)

FIGURE 15. Effect of different pavement temperatures: (a) pavement temperature of 42°C; (b) pavement temperature of 13°C.

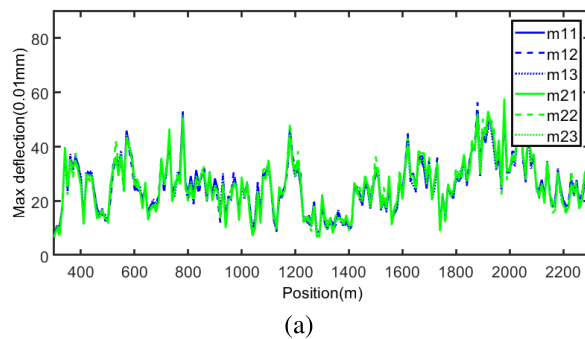
experiment, for which the correlation is 0.91 (42°C) and 0.95 (13°C).

### 3) COMPARISON WITH MULTIPLE CONTINUOUS DYNAMIC DEFLECTOMETERS

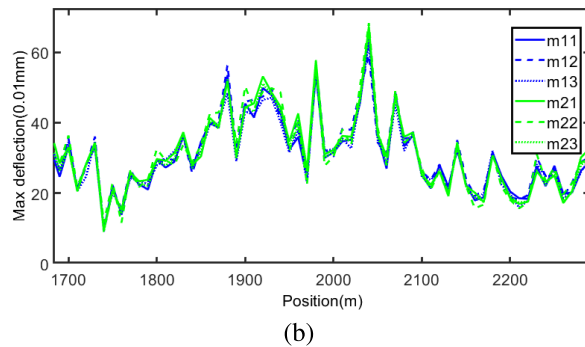
In dynamic deflection measurement, the TSD (Greenwood, Denmark) and the LDD (Zoyon, China) have achieved success in both theory and application. However, it is difficult to obtain the results of both deflectometers for the same pavement and the same period of time. Therefore, we chose multiple LDDs to analyze the consistency of their results in the same pavement and at the same period of time.

Figure 16 shows the results of two LDDs in the same pavement section, where three consecutive measurements were taken.  $m_{ij}$  represents the  $j$ -th measurement of device  $i$ . The results of the two LDDs on the same pavement are relatively consistent. The repeatability of the six measurements is 95%.

The autocorrelation of an individual LDD and the correlation of multiple LDDs are shown in Table 8.  $Avg_1$  is the



(a)



(b)

FIGURE 16. Autocorrelation and correlation of different LDDs on the measurement results: (a) entire experimental pavement section (300–2300 m); (b) part of the experimental pavement section (1685–2290 m).

average measurement result of device  $i$ . The autocorrelation of the individual LDD measurement results is higher than 0.98, and the correlation of the multiple LDDs is more than 0.98. It can therefore be concluded that the LDDs have a good and stable performance.

### V. CONCLUSION

In this article, we have shown that pavement roughness, vehicle speed, pavement temperature, and pavement structure have little influence on the repeatability of LDD measurements. The repeatability of the measurement results was more than 95% for the pavement with a mean deflection value of greater than 15 (0.01 mm). For the pavement with a mean deflection value of less than 15 (0.01 mm), the repeatability of the measurement was generally 80–95%, but the standard deviation of each measurement point was far less than the measured deflection basin. The correlation between the LDD and the FWD was slightly higher than that with the LDD and the BBD. However, all the correlations were over 0.90.

The correlation of the multiple LDDs under the same conditions was more than 0.95.

Through the review of the mechanism of the Euler-Bernoulli beam upon an elastic foundation and the corresponding influencing factors, this article has analyzed and summarized the internal and external factors causing the deviation of the dynamic deflection measurement. The effects of pavement temperature, vehicle speed, and pavement condition were corrected. Under the system limitations of pavement temperature (0–45°C) and vehicle speed (15–90 km/h), the deflection value is stable under the proposed correction method and is consistent with the reference value. However, the pavement will fuse or freeze at extreme temperatures, destroying the assumptions in the model. The same problem also affects the maximum vehicle speed. The upper speed limit of the revised model is set at 90 km/h, due to the limitation of the sensor (Doppler vibrometer). The proposed correction method for the continuous dynamic deflectometer is limited by the absence of a measuring technique for the pavement structure, subgrade humidity, and pavement thickness. The deflection basin is affected by the pavement structure and the condition of the pavement materials [32], so these factors should be considered in the future.

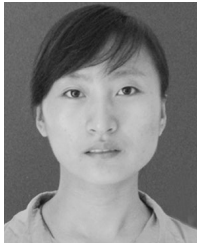
In spite of its limitations, this work certainly suggests that LDDs have strong robustness in different environments and conditions. The results will add to our understanding of velocity-based continuous dynamic deflection measurement.

## REFERENCES

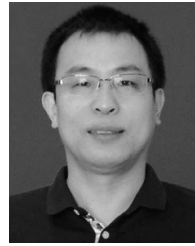
- [1] D. Liu, Z. Li, and Z. Lian, "Compaction quality assessment of earth-rock dam materials using roller-integrated compaction monitoring technology," *Autom. Construct.*, vol. 44, pp. 234–246, Aug. 2014.
- [2] Q. Xu and G. K. Chang, "Adaptive quality control and acceptance of pavement material density for intelligent road construction," *Autom. Construct.*, vol. 62, pp. 78–88, Feb. 2016.
- [3] L. Zhou, Q. Wu, and J. Ling, "Comparison of FWD and Benkelman beam in evaluation of pavement structure capacity," in *Proc. Paving Mater. Pavement Anal.*, 2010, pp. 405–411.
- [4] M. D. Nazzal and L. N. Mohammad, "Estimation of resilient modulus of subgrade soils using falling weight deflectometer," *Transp. Res. Record*, vol. 2186, no. 1, pp. 1–10, 2010.
- [5] K. Deblouis, J.-P. Bilodeau, and G. Dore, "Use of falling weight deflectometer time history data for the analysis of seasonal variation in pavement response," *Can. J. Civil Eng.*, vol. 37, no. 9, pp. 1224–1231, 2010.
- [6] D. Steele, J. Hall, R. Stubstad, A. Peekna, and R. Walker, "Development of a high-speed rolling wheel deflectometer," in *Proc. Pavement Eval. Conf.*, Roanoke, VA, USA, 2002, pp. 1–13.
- [7] D. S. Gedafa, M. Hossain, R. W. Miller, and D. Steele, "Network level pavement structural evaluation using rolling wheel deflectometer," *Transp. Res. Board 87th Annu. Meeting*, Washington, DC, USA, Tech. Rep. 08-2648, 2008.
- [8] P. Andrén, "Development and results of the Swedish road deflection tester," Ph.D. dissertation, School Archit. Built Environ., Byggetenskap, Stockholm, Sweden, 2006.
- [9] D.-H. Chen, B. H. Nam, and K. H. Stokoe, "Application of rolling dynamic deflectometer to forensic studies and pavement rehabilitation projects," *Transp. Res. Rec.*, vol. 2084, no. 1, pp. 73–82, 2008.
- [10] J. L. Y. Lee, "Improved rolling dynamic deflectometer testing and analysis procedures," Ph.D. dissertation, Civil Archit. Environ. Eng., Univ. Texas Austin, Austin, TX, USA, 2006.
- [11] G. Rada, J. Daleiden, and H. Yu, "Moving pavement deflection testing measurements," in *Proc. 48th Transp. Infrastruct. Conf.*, São Paulo, Brazil, 2010, pp. 1–16.
- [12] P. Andren and C. A. Lenngren, "Evaluating pavement layer properties with a high-speed rolling deflectometer," *Proc. SPIE*, vol. 3994, May 2000, pp. 192–201.
- [13] D. Steele, J. Hall, R. Stubstad, A. Peekna, and R. Walker, "Development of a high-speed rolling wheel deflectometer," *Revista Ingeniería de Construcción*, vol. 18, no. 2, pp. 79–85, 2003.
- [14] L. He, H. Lin, Q. Zou, and D. Zhang, "Accurate measurement of pavement deflection velocity under dynamic loads," *Autom. Construct.*, vol. 83, pp. 149–162, Nov. 2017.
- [15] S. Rasmussen, J. A. Krarup, and G. Hildebrand, "Non-contact deflection measurement at high speed," in *Proc. 6th Int. Conf. Bearing Capacity Roads, Railways Airfields*, vol. 8, 2002, pp. 1–8.
- [16] J. Krarup, S. Rasmussen, L. Aagaard, and P. G. Hjorth, "Output from the greenwood traffic speed deflectometer," in *Proc. 22nd ARRB Conf.*, Canberra, ACT, Australia, 2006, p. 10.
- [17] R. Soren, A. Lisbeth, B. Susanne, and K. Jorgen, "A comparison of two years of network level measurements with the traffic speed deflectometer," in *Proc. Transp. Res. Arena Eur.*, 2008, pp. 1–8.
- [18] E. O. Lukanen, R. Stubstad, R. C. Briggs, and B. Intertec, "Temperature predictions and adjustment factors for asphalt pavement," Turner-Fairbank Highway Res. Center, McLean, VA, USA, Tech. Rep. FHWA-RD-98-085, 2000.
- [19] *AASHTO Guide for Design of Pavement Structures*, AASHTO, Washington, DC, USA, 1993.
- [20] J. A. R. García and M. Castro, "Analysis of the temperature influence on flexible pavement deflection," *Construct. Building Mater.*, vol. 25, no. 8, pp. 3530–3539, 2011.
- [21] J. Weligamage, N. Piyatrapoomi, and L. Gunapala, "Traffic speed deflectometer—Queensland trial," *Queensland Roads*, vol. 9, pp. 16–27, Sep. 2010.
- [22] Q. Li, Q. Zou, Q. Mao, X. Chen, and B. Li, "Efficient calibration of a laser dynamic deflectometer," *IEEE Trans. Instrum. Meas.*, vol. 62, no. 4, pp. 806–813, Apr. 2013.
- [23] A. F. Bissada and H. Guirguis, "Temperature dependency of dynamic deflection measurements on asphalt pavements," *Transp. Res. Rec.*, no. 930, pp. 57–59, 1983. [Online]. Available: <https://trid.trb.org/Results?txtKeywords=Temperature+dependency+of+dynamic+deflection+measurements+on+asphalt+pavements#/View/203378>
- [24] M. Nasimifar, R. V. Siddharthan, G. R. Rada, and S. Nazarian, "Dynamic analyses of traffic speed deflection devices," *Int. J. Pavement Eng.*, vol. 18, no. 5, pp. 381–390, 2017.
- [25] Y. L. Ye, C. Y. Zhuang, and R. F. Zhang, "A method for temperature correction of HMA dynamic modulus," in *Appl. Mech. Mater.*, vols. 178–181, pp. 1615–1618, May 2012.
- [26] *Specifications for Design of Highway Asphalt Pavement*, Standard JTG D50-2017, Ministry of Transport of the People's Republic of China, 2017, pp. 45–46.
- [27] K. Shrp, "SHRP procedure for temperature correction of maximum deflections," PCS/Law Eng., Washington, DC, USA, Tech. Rep. SHRP-P-654, 1993.
- [28] Y. Zheng, P. Zhang, and H. Liu, "Correlation between pavement temperature and deflection basin form factors of asphalt pavement," *Int. J. Pavement Eng.*, vol. 20, no. 8, pp. 874–883, 2019.
- [29] D.-H. Chen, J. Bilyeu, H.-H. Lin, and M. Murphy, "Temperature correction on falling weight deflectometer measurements," *Transp. Res. Rec.*, vol. 1716, no. 1, pp. 30–39, 2000.
- [30] Y. R. Kim, B. O. Hibbs, and Y.-C. Lee, "Temperature correction of deflections and backcalculated asphalt concrete moduli," in *Proc. Transp. Res. Rec.*, no. 1473, 1995, pp. 55–62.
- [31] A. Jitin, V. Tandon, and S. Nazarian, "Continuous deflection testing of highways at traffic speeds," Univ. Texas, El Paso, TX, USA, Tech. Rep. FHWA/TX-06/0-4380-1, 2006. [Online]. Available: <https://trid.trb.org/view/803160>
- [32] G. Salt, "Pavement deflection measurement and interpretation for the design of rehabilitation treatments," *Transit New Zealand Rep.*, no. 117, p. 70, 1998. [Online]. Available: <https://trid.trb.org/view/507372>



**JIANGHAI LIAO** received the B.E. degree in communication engineering and the M.E. degree in pattern recognition and intelligent systems from Shenzhen University, Shenzhen, China, in 2007 and 2010, respectively, where he is currently pursuing the doctoral degree with the Guangdong Key Laboratory of Urban Informatics. His research interests include acquisition and analysis of infrastructure status information.



**HONG LIN** is currently pursuing the Ph.D. degree in signal and information processing, with the Electronic Information School, Wuhan University, Wuhan, China. Her research interests include pavement nondestructive measurement and pavement disease detection.



**DEJIN ZHANG** received the master's degree in computer software and theory from the Huazhong University of Science and Technology, Wuhan, China, in 2004, and the Ph.D. degree in photogrammetry and remote sensing from Wuhan University, Wuhan, in 2012. He is currently a Professor with Shenzhen University, Shenzhen, China. His research interests include pavement nondestructive measurement and intelligent transportation system.

• • •



**QINGQUAN LI** received the Ph.D. degree in GIS and photogrammetry from the Wuhan Technical University of Surveying and Mapping, China, in 1998. From 1988 to 1996, he was an Assistant Professor with Wuhan University, where he became an Associate Professor, in 1996, and has been a Professor, since 1998. He is currently the President and a Professor of Shenzhen University, China; a Professor with the State Key Laboratory of Information Engineering in Surveying, Mapping and Remote Sensing, Wuhan University; and the Director of Shenzhen Key Laboratory of Spatial Smart Sensing and Service. His research areas include intelligent transportation systems, 3D and dynamic data modeling, and pattern recognition. He is an Academician of International Academy of Sciences for Europe and Asia (IASEA); an Expert in Modern Traffic with the National 863 Plan and an Editorial Board Member of the *Surveying and Mapping Journal* and the *Wuhan University Journal — Information Science Edition*.